

UC Davis

UC Davis Previously Published Works

Title

PG545 enhances anti-cancer activity of chemotherapy in ovarian models and increases surrogate biomarkers such as VEGF in preclinical and clinical plasma samples

Permalink

<https://escholarship.org/uc/item/5s2961bt>

Journal

European Journal of Cancer, 51(7)

ISSN

0959-8049

Authors

Winterhoff, Boris
Freyer, Luisa
Hammond, Edward
[et al.](#)

Publication Date

2015-05-01

DOI

10.1016/j.ejca.2015.02.007

Peer reviewed



Published in final edited form as:

Eur J Cancer. 2015 May ; 51(7): 879–892. doi:10.1016/j.ejca.2015.02.007.

PG545 enhances anti-cancer activity of chemotherapy in ovarian models and increases surrogate biomarkers such as VEGF in preclinical and clinical plasma samples

Boris Winterhoff^{#1,†}, Luisa Freyer^{#2}, Edward Hammond^{#3}, Shailendra Giri⁴, Susmita Mondal², Debarshi Roy², Attila Teoman¹, Sally A. Mullany⁵, Robert Hoffmann², Antonia von Bismarck², Jeremy Chien⁶, Matthew S. Block⁷, Michael Millward⁸, Darryn Bampton³, Keith Dredge^{#,3}, and Viji Shridhar^{#,2}

¹Mayo Clinic, Department of Obstetrics and Gynecology, Division of Gynecologic Oncology, Minnesota, USA

²Mayo Clinic College of Medicine, Department of Experimental Pathology, Minnesota, USA.

³Progen Pharmaceuticals Ltd, Brisbane, Queensland, Australia.

⁴Henry Ford Health System, Neurology Research, Detroit, MI, USA.

⁵University of Minnesota, Department of Obstetrics and Gynecology, Division of Gynecologic Oncology, Minnesota, USA.

⁶Department of Cancer Biology, University of Kansas Cancer Center, Kansas City, Kansas, USA.

⁷Mayo Clinic College of Medicine, Department of Medical Oncology, Minnesota, USA.

⁸Department of Medical Oncology, Sir Charles Gairdner Hospital & University of Western Australia.

These authors contributed equally to this work.

Abstract

Background—Despite the utility of antiangiogenic drugs in ovarian cancer, efficacy remains limited due to resistance linked to alternate angiogenic pathways and metastasis. Therefore, we investigated PG545, an anti-angiogenic and anti-metastatic agent which is currently in Phase I clinical trials, using preclinical models of ovarian cancer.

Methods—PG545's anti-cancer activity was investigated *in vitro* and *in vivo* as a single agent, and in combination with paclitaxel, cisplatin or carboplatin using various ovarian cancer cell lines and tumour models.

#Corresponding authors: Viji Shridhar and Keith Dredge are senior corresponding authors. Viji Shridhar, Department of Experimental Pathology, Mayo Clinic, 200 1st St. SW, Rochester, MN, 55905, Tel.: +1 507 266 2775, Fax: +1 507 284 1678, shridhar.vijayalakshmi@mayo.edu or Keith Dredge, Progen Pharmaceuticals Ltd., 2806 Ipswich Road, Darra, Brisbane, Queensland 4076, Australia. Tel.: +61 7 3273 9179, keithd@progen-pharma.com.

†Current Affiliation: Department of Obstetrics, Gynecology and Women's Health, University of Minnesota, USA.

Conflicts of interests: Edward Hammond, Keith Dredge and Darryn Bampton are employed by, or act as consultants for Progen Pharmaceuticals, which developed PG545. None of the other authors have any conflicts of interest.

Results—PG545, alone, or in combination with chemotherapeutics, inhibited proliferation of ovarian cancer cells, demonstrating synergy with paclitaxel in A2780 cells. PG545 inhibited growth factor-mediated cell migration and reduced HB-EGF-induced phosphorylation of ERK, AKT and EGFR *in vitro* and significantly reduced tumour burden which was enhanced when combined with paclitaxel in an A2780 model or carboplatin in a SKOV-3 model. Moreover, in the immunocompetent ID8 model, PG545 also significantly reduced ascites *in vivo*. In the A2780 maintenance model, PG545 initiated with, and following paclitaxel and cisplatin treatment, significantly improved overall survival. PG545 increased plasma VEGF levels (and other targets) in preclinical models and in a small cohort of advanced cancer patients which might represent a potential biomarker of response.

Conclusion—Our results support clinical testing of PG545, particularly in combination with paclitaxel, as a novel therapeutic strategy for ovarian cancer.

Keywords

PG545; ovarian cancer; tumour microenvironment; heparanase; VEGF; HB-EGF

Introduction

Significant progress in understanding the molecular biology of epithelial ovarian cancer (OVCA), has not yet translated into improvements in disease outcomes. Most patients respond initially to therapy, however the majority relapse, making OVCA essentially incurable [1]. As a result, efforts are ongoing to identify novel agents that target the tumour microenvironment to impact angiogenesis, invasion and metastasis. While antiangiogenic therapy is emerging as a viable option for OVCA, other growth factors either remain functionally active or increase as a mode of resistance to anti-VEGF therapies [1]. The resistance mechanisms associated with the use of anti-VEGF therapies have been reported to include FGF-2 [2] and HB-EGF [3]. Therefore, a more effective treatment strategy would be to target key angiogenesis pathways simultaneously whilst reducing metastatic spread *via* inhibition of heparanase, an enzyme whose expression correlates with poor survival in metastatic gynecological adenocarcinomas [4] and may contribute to the proliferation and metastasis of ovarian cancer [5]. Heparan sulfate proteoglycans (HSPG) play an important role in modulating heparan sulfate-binding growth factor (GF) signaling and heparanase activity [6,7], in the extracellular matrix [8], and are implicated in angiogenesis and metastasis [9–11]. Thus, the development of therapeutics that inhibit these growth factors plus heparanase activity may have an advantage over existing antiangiogenic agents [12].

PG545 is a sulfated tetrasaccharide optimized for potency through the addition of a lipophilic moiety to attain potent *in vivo* activity, long plasma half-life and low anticoagulant potential [13,14]. It inhibits angiogenesis *via* inhibition of VEGF and FGF-2 while preventing metastasis through blockade of heparanase [13,15]. PG545 inhibits *in vivo* angiogenesis, attenuates tumour growth and/or metastasis in various cancer models including lung, hepatocellular, prostate, colon, melanoma, pancreatic and head and neck cancers [16,17]. In a skin carcinogenesis model, PG545 inhibited the heparanase-dependent formation of tumour lesions providing further validation for the targeting of this enzyme in the development of cancer therapeutics [18]. It also reduced heparanase expression in a

model of metastatic breast cancer [17]. However, PG545 activity in OVCA has not yet been studied. This is particularly relevant as previous investigations supporting the efficacy of anti-angiogenic agents in OVCA [19–21] would suggest an additional treatment benefit could be achieved with dual targeting of the angiogenic (VEGF) and metastatic (heparanase) pathways. Therefore, the aim of this study was to investigate the activity of PG545 in OVCA by, firstly, studying its impact on ovarian tumour cell growth, cellular migration and invasion, secondly, further define the molecular downstream signaling effects of PG545, and, thirdly, explore the impact of PG545 as a single agent and in combination with cytotoxic therapy in OVCA preclinical models. Finally, a preliminary assessment of putative biomarkers for PG545 activity was performed by analyzing GFs and heparanase in the plasma samples from mice and a small cohort of advanced cancer patients treated with PG545 from a previous Phase I trial ([ClinicalTrials.gov](https://clinicaltrials.gov/ct2/show/study/NCT01252095) Identifier: NCT01252095). The safety and tolerability of intravenously-infused PG545 is currently being assessed in patients with advanced solid tumours ([ClinicalTrials.gov](https://clinicaltrials.gov/ct2/show/study/NCT02042781) Identifier: NCT02042781).

Materials and Methods

Cell Culture

SKOV3, OV202, A2780, and ID8 cells were cultured as previously described [22,23]. A2780 cells were obtained from Fox Chase Cancer Center and ID8 cells from Dr. Katherine Roby [24].

Growth Factors & Reagents

HB-EGF, HGF, FGF-2, VEGF, SDF-1, FGF-2, human recombinant VEGF₁₆₅, stromal cell-derived factor-1 were purchased from R&D Systems (Minneapolis, MN). PG545 was synthesized by Progen Pharmaceuticals (Brisbane, QLD, Australia). All drugs (PG545, cisplatin (Calbiochem, Millipore, Billerica, MA), carboplatin (50mg/5ml, Novaplus, Novation, Irvine, TX), paclitaxel (30mg/5ml, Hospira, Lake Forest, IL) were dissolved using cell culture medium for *in vitro* experiments and phosphate buffered saline (PBS) for *in vivo* studies.

Cell viability assays and in vitro drug combination assay between paclitaxel and PG545

To evaluate the effect of PG545, cisplatin and/or paclitaxel on cell viability, 3000 A2780 or SKOV3 cells in replicates of 5 were plated in a 96 well plate and treated with increasing concentrations of each drug for 48h. The MTT assay was performed as previously described (22). To determine the synergy between paclitaxel and PG545, cell viability was determined using MTT assay in A2780 cells. Briefly, IC₅₀ of paclitaxel and/or PG545 alone were determined initially. To determine if PG545 acts synergistically with paclitaxel, constant ratio synergy studies were performed using the Chou-Talalay method and the combination index (CI) and dose reduction index (DRI) were calculated using CalcuSyn software (Biosoft, USA). CI values between 0.1-0.3 indicate extremely strong synergism, 0.3-0.7 indicates strong synergism; 0.7-0.85, moderate synergism; 0.85-0.9, slight synergism; 0.9-1.10, approximately additive effect and values above this indicate antagonism. The DRI is a measure of how much the dose of each drug may be reduced at a given effector level compared with the doses of each drug alone; values of greater than one indicate that the drug

dose can be reduced for the same effect and the larger the DRI the greater the dose reduction possible [25].

Wound Healing Scratch Assay

90% confluent 1×10^5 SKOV3 cells grown and maintained in 0.2% serum-containing medium were scratched with a 200 μ l pipette tip. Stimulatory growth factors (HB-EGF at 50ng/ml, HGF at 50ng/ml, FGF-2 at 1ng/ml, VEGF at 10ng/ml, or SDF-1 at 50ng/ml) were added to the medium in the presence or absence of PG545 at 5 μ M. The rate of wound closure was calculated as previously described [23].

Fluorometric Invasion Assay

SKOV3 cells (1×10^5) were seeded into FIA chambers (CORNING, Corning, NY). The outer chamber contained the chemo-attractant (fetal bovine serum and/or 50 ng/mL HB-EGF). The chamber was incubated for 72hrs allowing cells to pass through the Matrigel layer onto the surface of a fluorescence-blocking membrane. Cells were labeled with calcein-AM solution (Life Technologies, Carlsbad, CA) for 60 minutes. Fluorescence of the invaded cells was then measured according to the manufacturer's instructions. SKOV3 cell invasion was measured with or without chemo-attractant in the presence or absence of PG545.

HB-EGF Induced Signaling by Western Blot Analysis

SKOV3 and OV202 cells were cultured in 0.2% serum containing medium for 12h. 50ng/ml HB-EGF was added with and without 5 μ M PG545 for 5, 10, 20, 40, and 60 minutes. Cell lysates were analyzed by Western blotting with antibodies from Cell Signaling (Danvers, MA): EGFR, phosphorylated EGFR (p-EGFR; Tyr¹⁰⁶⁸), AKT, phosphorylated AKT (p-AKT; Ser⁴⁷³), ERK, and phosphorylated ERK (p-ERK). Experiments were repeated three times. Densitometric analysis using Scion Image software was performed.

Tumour Models and Drug Administration

All animal protocols were reviewed and approved by the Institutional Animal Care and Use Committee of Mayo Clinic (ID8, the MIR Discovery and Imaging Services, Ann Arbor's (DIS-AA) Animal Care and Use Committee (A2780 s.c. model) and the University of Adelaide Animal Ethics Committee (SKOV3 model). The mice were housed in an appropriate pathogen-free facility and had *ad libitum* access to food and water, following all guidelines for the proper and humane use of animals in research. Female mice (C57/BL6, CrI:NU-Foxn1^{nu}, SCID (C.B-17-Igh-1^b-Prkdc^{scid}) between the ages of 6-8 weeks were obtained from the NCI (Fredericksburg, MD), Harlan Laboratories (Indianapolis, IN), Charles River (Piedmont, NC) and University of Adelaide (SA, Australia). C57BL/6 mice were injected i.p. with 1×10^7 ID8 cells. Treatment commenced on Day 3 with 20mg/kg PG545 i.p. twice weekly or weekly (ID8).

In A2780 studies, PG545 was administered via the intravenous (i.v.) or subcutaneous (s.c.) route once tumours reached an estimated mass of approximately 140 mg s.c. after implantation of 30-60mg A2780 tumour fragments using an 11-gauge trocar needle or via s.c. injection of 1×10^7 cells. PG545 was administered s.c. or i.v. at 20mg/kg s.c. weekly

versus 7.5mg/kg i.v. twice weekly versus 15mg/kg i.v. once weekly. After 3 weeks of treatment tumour volume and overall survival was assessed.

To determine the efficacy of PG545 in combination, mice were treated with weekly paclitaxel alone (15mg/kg, i.v.), PG545 (20mg/kg, s.c.) or a combination of paclitaxel (15mg/kg, i.v.) followed two days later by PG545 (20mg/kg, s.c.). In the SKOV3 model, 5×10^6 cells were injected s.c. and SCID mice were treated with single agent carboplatin at 40mg/kg, PG545 (dose reduction from 20 to 10mg/kg after the first week), or PG545 plus carboplatin, once tumours reached a volume of 123mm³. Using the immunocompetent luciferase-expressing ID8 model, mice were injected i.p. with 5×10^6 cells. Treatment started at day 3: PG545 20mg/kg weekly for 10 weeks (i.p.). Weekly bioluminescent reporter imaging was performed to monitor the seeding of ID8-luc cells, using the Xenogen IVIS 200 System. Twelve weeks after inoculation, all mice were sacrificed [20].

In the A2780 maintenance model, 1.25×10^6 cells were injected i.p. into SCID mice, treatments were given i.p. Mice were randomly assigned to 5 different treatment groups: a control group, a single PG545 group, a cisplatin and paclitaxel group, a cisplatin, paclitaxel and PG545 (with PG545 starting at day 3) group and cisplatin, paclitaxel and PG545 (with PG545 starting at day 10) group.

Preclinical Pharmacodynamic Assessment

VEGF was measured from samples obtained in the ID8 (ascites and plasma at day 60, and 4 days following last PG545 treatment) and A2780 model (plasma, at times indicated in results section). Blood was collected in heparin coated tubes from three mice at necropsy. Plasma was obtained by separating cells by centrifugation. Ascites and plasma VEGF (ID8) was measured using a MesoScale Discovery ELISA (Rockville, MD). VEGF concentrations were measured in the plasma of nude mice (A2780 model) using a mouse ELISA kit ELISA kit (R&D Systems).

Preclinical Pharmacokinetic Assessment

PG545 concentrations in plasma were measured using a LC/MS assay as previously described [16]. For the 7.5mg/kg twice weekly i.v. dose and 15mg/kg once weekly i.v. dose, the sampling times were 10min, 30min, 2h, 4h, 8h, 24h, 48h and 96h post-dose. For the 20mg/kg once weekly s.c. dose, the sampling times were 1h, 4h, 8h, 24h, 48h, 96h, 120h and 168h post-dose. The pharmacokinetic parameters, C_{max} (maximum plasma concentration), T_{max} (time of maximum plasma concentration), $t_{1/2}$ (half-life), and AUC (area under the concentration versus time curve) were derived from the mean plasma PG545 concentration versus time data using model independent methods.

Phase I Clinical Trial

Four patients with advanced solid tumours were treated with PG545 via s.c. administration in a Phase I study (NCT01252095). The trial was conducted in accordance with a Human Research Ethics Committee (HREC)-approved protocol and patient consent. Unexpected local injection site reactions halted the trial, plasma VEGF and heparanase levels were

measured using ELISA (R&D Systems and InSight Biopharmaceuticals). Blood samples were obtained pre-dose, 2h, 4h, 8h, 24h, 72, 96h, 120h and 168h post-dose.

Statistical Analysis

Two-tailed, unpaired Student's t-test and one-way ANOVA with Bonferroni correction or a Newman-Keuls multiple comparisons test as a *post hoc* test were used. Survival was analyzed by the Kaplan-Meier method. For analysis of survival data, the Log-rank (Mantel-Cox) and Gehan-Breslow-Wilcoxon tests were employed to analyse the significance between individual survival curves which was reported following adjustment using the Bonferroni corrected threshold method for multiple comparisons. All statistical analyses were performed with Prism (GraphPad Software, La Jolla, CA).

Results

PG545 inhibits OVCA cell viability in vitro as single agent and in combination with chemotherapeutic agents

The potential of PG545 to synergise with the chemotherapeutic agents cisplatin and paclitaxel against OVCA cells was investigated using cell viability assays. Firstly, we showed that PG545 exhibited concentration-dependent growth inhibition (Supplementary Fig. 1A and D) in A2780 and SKOV3 cell lines. In combination with cisplatin or paclitaxel, PG545 at 10 μ M increased the cytotoxic effect of cisplatin or paclitaxel over a range of concentrations in A2780 and SKOV3 cell lines (Supplementary Fig. 1B, C, E and F). The most pronounced effect was seen in the A2780 cells treated with paclitaxel and PG545 (Supplementary Fig. 1C).

The concentrations for the combination experiment were determined based on the individual dose response assay with PG545 and paclitaxel in A2780 cells (Supplementary Fig. 1A and C). Paclitaxel exhibited 50% growth inhibition after 48h of treatment at 760 nM, while PG545 alone showed concentration-dependent growth inhibition at a range of 10-160 μ M in A2780. The combined action of paclitaxel and PG545 at a constant ratio showed extremely strong synergy as the Combination Index (CI) values were 0.088 and 0.034 at 0.75 and 0.95 fraction affected (Fa). The Fa variable denotes the relative completion of the biological process in question: in this case 0.75 indicates that tumour cell growth has been inhibited by 75%. Of note, synergy was demonstrated across nearly the entire range of the drug concentrations and Fa values (Fig. 1A). The combination data were next analysed to determine the dose reduction indices (DRI) for PG545 and paclitaxel. DRI values greater than one indicate that the drug dose can be reduced for the same affect and the larger the DRI the greater the dose reduction possible. The results for PG545 and paclitaxel show high DRI for both compounds, particularly at the higher Fa (Fig. 1B). This has clinical significance because it suggests that the synergistic interaction between these two agents may allow their doses to be modulated downwards, thus diminishing toxicity.

PG545 Inhibits GF-Induced Cell Migration and Invasion in vitro

The effect of PG545 on GF induced migratory capacity of SKOV3 cells was measured using a scratch assay. Universally, PG545 significantly inhibited the migration of SKOV3 cells

regardless of the type of growth factor present (Fig. 2A and B). Similarly, PG545 significantly inhibited HB-EGF-induced invasion of SKOV3 cells as assessed by the Fluorometric Invasion Assay. (Fig. 2C).

PG545 Modulates HB-EGF Induced Signaling in OVCA Cells

Serum starved SKOV3 and OV202 cells stimulated with HB-EGF showed phosphorylation of EGFR at Tyr 1068, AKT (ser473) and MAPK (p-ERK) in the absence of PG545. However, PG545 treatment resulted in a significant decrease in the activation, occurring within 5 minutes of PG545 exposure for p-EGFR and AKT in both cell lines and 10 minutes for p-ERK (Fig. 2D and E) respectively.

Effect of PG545 as a single agent in subcutaneous Preclinical Models of OVCA

To further assess PG545 dosing schedule and tumour response in mouse models, we injected A2780 cells subcutaneously. The control group was compared to three different treatment groups. The first group received 20mg/kg s.c. once a week for 3 weeks. The second treatment group received 7.5mg/kg i.v. twice a week for 3 weeks and the third group was treated with 15mg/kg i.v. once a week for 3 weeks. All treatment groups had significantly smaller tumours than the control group with volumes less than half that of the control group after 12 days of treatment (Fig. 3A). Median survival for all the treatment groups were significantly higher compared to the control group that had a median survival of 9 days (Fig. 3B).

Combination Therapy Activity in subcutaneous models of A2780 and SKOV3

We further assessed the activity of PG545 in combination with standard OVCA chemotherapeutic agents: paclitaxel in the A2780 model and carboplatin in the SKOV3 model. In the A2780 model, three treatment groups were compared to the untreated control group. The first group was treated with i.v. paclitaxel at a dose of 15mg/kg once weekly. The second group was treated with PG545 20mg/kg s.c. once weekly and the third group was treated with the combination of PG545 at 20mg/kg and paclitaxel. Two days post-paclitaxel treatment, PG545 was administered and treatment continued for two weeks, after which, the first group treated with paclitaxel had an 11% Tumour Growth Inhibition (TGI) when compared to the control group. PG545 as a single agent demonstrated a statistically significant TGI of 48% compared to the control group. The combination of paclitaxel and PG545 had a statistical significant TGI of 79% when compared to the control group and when compared to the paclitaxel group (Fig. 3C).

Combination of PG545 (s.c.) and carboplatin (i.v.) was tested in the moderately platinum-sensitive SKOV3 model comparing the vehicle control with three treatment groups: PG545 dosed at 20mg/kg followed by 10 mg/kg (20/10mg/kg) once weekly, carboplatin 40 mg/kg once weekly and a combination of 20/10mg/kg PG545 and 40mg/kg carboplatin. By day 19, TGI was estimated at 40% for PG545 alone, 43% carboplatin alone and 58% for the combination. The PG545 group and PG545 in combination with carboplatin reached statistical significance (Fig. 3D).

PG545 activity in syngeneic mouse model of ovarian cancer

Next, to determine *in vivo* anti-tumour activities of PG545 in an immune intact, site-appropriate model system, PG545 was tested in the syngeneic immunocompetent intraperitoneal ID8 model. Treatment was started at day 3 after ID8 cell injection. The control group was compared to PG545 treatment group. The treatment group was treated with PG545 20mg/kg twice a week for the first week and then reduced to once a week for a total of 10 weeks. At 10 weeks, the abdominal circumference, ascites volume and macroscopic tumour weight were compared between each treatment group and the control group. Abdominal circumference was highest in the control group with a mean of 9.9cm and lower in the PG545 group with 7.4cm. Ascites volume was highest in the control group with 12ml and lower in the PG545 group with 4ml. The control group had measurable macroscopic tumour at necropsy with a mean tumour weight of 0.16g, while there was no measurable tumor in the PG545 treated mice, all findings were statistically significant (Fig. 4A). The ID8 cells were transfected with luciferase allowing the tumour burden to be visualized throughout the treatment. Fig. 4B confirms visually the findings of reduced tumour burden in mice treated with PG545 compared to the control group at 2 weeks of treatment and 9 weeks respectively.

Combination Maintenance Therapy Activity in an intraperitoneal A2780 model of ovarian cancer

To determine the potential role of PG545 as a maintenance drug, an A2780 i.p SCID mouse model was used. Ten mice were randomly assigned to 5 different treatment groups, including a control untreated group, PG545 group, cisplatin and paclitaxel group, cisplatin, paclitaxel and PG545 (with PG545 starting at day 3) group and cisplatin, paclitaxel and PG545 (with PG545 starting at day 10) group (Fig. 5A). The lowest median overall survival (OS), was observed in the control group with 23 days, followed by the PG545 only group with 43 days (Fig. 5B and C). The cisplatin paclitaxel group had a Median OS of 46 days. The maintenance PG545 groups had the best median OS with 58 days for the group that started PG545 at 10 days, while the median OS was not reached at 62 days for the group that started PG545 at day 3; the differences in median OS were statistically significant ($p < 0.001$). The study was terminated at day 62 by which stage only 2/10 mice in the control group, 1/10 in the PG545 group, 3/10 in the cisplatin paclitaxel group, 3/10 in the PG545 maintenance group starting at day 10 but 9/10 mice in the group starting PG545 at day 3 survived and had no visible evidence of tumour formation. The anti-tumour activity correlated with significant reductions in tumour cell proliferation (as determined by Ki67 staining), and microvessel density (as determined by CD31 expression) following administration of PG545 in combination with cisplatin and paclitaxel compared with either treatments alone (Figure S2).

PG545 modulates VEGF in vivo

In the ID8 syngeneic model, VEGF levels were elevated two-fold in the plasma of PG545-treated mice, reaching borderline significance ($p = 0.06$) (Fig. 6A). In contrast, the levels of VEGF in ascites were higher in the control mice compared to the PG545 treated animals (Fig S3). It is also noteworthy that the levels of VEGF in the ascites (400-700 pg/mL) are far

higher than in plasma (10-25 pg/mL). The effect of PG545 on plasma VEGF in the ID8 model was further substantiated when similar findings were apparent in the A2780 model (Fig. 6B-D). In addition to modulating plasma VEGF, PG545 also modulated the concentration of plasma heparanase in the A2780 model (Fig. S4).

PG545 increases plasma levels of VEGF in patients with solid tumours

Four patients with recurrent solid tumours were treated with PG545 (either 25 or 50mg, s.c. once weekly). PG545 concentrations and the levels of various target proteins over time were measured in the plasma of these patients. Patient 003 with thyroid cancer (total treatment of 2 weekly 50mg doses) exhibited a 2-fold increase in plasma VEGF levels after the first dose (Fig. 7A). In contrast, Patient 021 (total treatment of 7 weekly 25mg doses) with colon cancer had an increase in plasma VEGF levels peaking at 1.7-fold after the final dose (Fig. 7B). Patient 022 (total treatment of 3 weekly 25mg doses) with pancreatic cancer displayed a 1.8-fold increase in plasma VEGF levels after 28 days, returning to baseline after a further 28 days without PG545 treatment (Fig. 7C). Finally, Patient 023 with melanoma (total of 8 weekly 25mg doses) demonstrated a 3.5-fold increase of VEGF plasma levels after 22 days of treatment with PG545 (Fig. 7D). With the exception of VEGF in Patient 021, all of the analytes returned, approximately, to the pre-dosing baseline levels after PG545 administration had ceased indicating that the perturbations were transient in nature. Similar results were observed with other target proteins of PG545 including FGF-2 (Fig. S5), HB-EGF (Fig. S6) and heparanase (Fig. S7). Apart from HB-EGF in the thyroid and pancreatic patients, all other markers showed some response in all of the patients.

PG545 pharmacokinetic profile in tumour-bearing mice and advanced cancer patients

Plasma concentration versus time curves for the A2780 model and advanced cancer patients are represented in Figure 6 and Figure 7 respectively. A comparison of basic pharmacokinetic parameters in the A2780, SKOV3 models and advanced cancer patients is available in supplementary data (Table S1). Two key points are highlighted here. First, the A2780 data suggests that AUC (as opposed to C_{max}) is the relevant measure of exposure to associate with anti-tumour activity because a low dose given i.v. twice-weekly exhibited similar efficacy to a high dose given i.v. (or s.c.) once-weekly. Second, assuming exposure is proportional with increasing dose levels, the data suggest that to achieve therapeutic levels in human subjects, the efficacious s.c. dose would be approximately 150mg (likely lower for i.v. dosing due to 100% bioavailability).

Discussion

Multiple clinical trials have demonstrated efficacy of the antiangiogenic drug bevacizumab, in the treatment of advanced OVCA [19–21]. However, despite initial responses, once bevacizumab treatment was stopped, most patients recurred which resulted in bad prognosis. Genomic and molecular complexity of epithelial OVCA and its ability to metastasise via multiple routes (intraperitoneal, hematogenous, lymphatic) might contribute to some of the resistance against single target anti angiogenic treatments, like bevacizumab [19–21,26]. Thus, current attempts are focusing on the development of anti-cancer therapy to determine the optimal combinations of stromal-targeting agents with conventional chemotherapy to

target multiple pathways and hallmarks of epithelial OVCA simultaneously [27,28]. PG545 is now considered a regulator of the tumour microenvironment due to effects on multiple cell types and targets that constitute solid tumours [16,17,29] and is currently being investigated as a 1-hour intravenous infusion administered once-weekly in a Phase I trial in advanced cancer patients. Epithelial OVCA provides a particularly relevant target for PG545 due to known activity of the VEGF and HB-EGF angiogenic pathways in the molecular pathogenesis of OVCA, as well as the high metastatic potential; both contributing to the high mortality of this disease [30]. Tang and colleagues showed anti-tumour activity of an HB-EGF inhibitor CRM197 in platinum-resistant ovarian cancer cells [31].

While PG545 demonstrated efficacy in solid tumours including melanoma, breast, colon, lung, liver and pancreas [13,15–17], but the activity of PG545 or its potential to inhibit VEGF and HB-EGF in OVCA has not been assessed. Independent of the type of GF used to stimulate the SKOV3 cells, exposure to PG545 resulted in the inhibition of cellular migration, invasive capacity and growth factor mediated signaling, providing support for the action of PG545 against GF. This complements previous *in vivo* data documenting the antimetastatic activity of PG545 in other tumour types [13,15–17] and confirming that the antiangiogenic/antimetastatic effects of PG545 are, at least partly, facilitated through its ultimate effects on signaling pathways including ERK/MAPK and AKT.

Regardless of the route of PG545 administration and the location of tumour (subcutaneous or intraperitoneal), single agent PG545 had significant anti-tumour activity in both the cisplatin sensitive A2780 and SKOV3 models. This anti-tumour activity was also demonstrated in the syngeneic immunocompetent ID8 mouse model, when once-weekly PG545 monotherapy completely inhibited tumour growth and significantly reduced ascites accumulation. Thus, our *in vivo* data demonstrates that single agent PG545 may exert comparable anti-tumour activity to standard chemotherapeutic agents used in the treatment of OVCA. In addition to its single agent activity, PG545 demonstrated synergy with paclitaxel *in vitro*, significantly reduced tumour growth when co-administered with paclitaxel (and carboplatin) *in vivo*, and significantly improved overall survival as a maintenance therapy following paclitaxel and cisplatin chemotherapy. These findings are particularly important as it highlights the potential utility for PG545 with paclitaxel or even in a maintenance setting as previously reported for bevacizumab with paclitaxel and cisplatin [32,33].

Plasma levels of VEGF, HB-EGF, FGF-2, which have all been linked to poor prognosis in ovarian cancer, and heparanase were increased in mice and patients treated with PG545 (Supplementary Fig S4-7). This represents preliminary evidence of target modulation, especially in patients, considering the doses used could be considered sub-therapeutic (no RECIST responses were observed in the trial PG545101), when comparing exposure (AUC) levels of efficacious doses from the preclinical ovarian models which were 2-4 fold higher than those measured in patients (Table S1). Blocking the interaction of VEGF (or other growth factors) and heparanase with HS within the tumour microenvironment may lead to a liberation of free ligand into the plasma. This would prevent VEGF-induced activation of cellular signaling (possibly via downregulation of the ERK/MAPK pathway, based on our *in vitro* data) in tumour endothelial cells, inhibit heparanase-mediated degradation of the ECM

and would lead to increases in plasma levels of these HS binding proteins. Similar increases in plasma VEGF concentration have been observed following treatment with bevacizumab [34]. Modeling studies have attributed these increases to depletion of VEGF from the tumour interstitium which, consequently, prevents this population of VEGF molecules from promoting tumour growth [34]. The pharmacodynamic response to PG545 in animal studies revealed two peaks in plasma HS binding proteins: the first just after dosing which may be due to a response in peripheral blood (e.g. platelets) or vasculature, while the second peak may represent a consequence of target modulation within the tumour microenvironment.

Since the generation of malignant ascites in ovarian cancer has been largely attributed to increased vascular permeability resulting from expression of VEGF by tumour cells, it seems likely that PG545 inhibition of VEGF in the peritoneal cavity leads to the reduction in ascites volume seen in PG545-treated mice (Fig. 4B) and significantly reduced VEGF levels in the ascites, when compared to the control group (Fig. S3). Similar decreases of ascites have been seen in ovarian cancer patients treated with bevacizumab [35,36]. The apparent contradiction between the PG545-associated increased plasma VEGF and decreased ascites VEGF levels can be understood by examining the relative concentrations in these two compartments and how they affect each other. VEGF levels in ascites were over ten-fold higher than the levels found in plasma indicating that leakage of plasma into the intraperitoneal space will have little effect upon ascites VEGF concentration. The main driver of VEGF levels in ascites is that secreted by tumour, stromal and immune cells [37] and, therefore, it appears likely that PG545-mediated suppression of one, or a combination, of these cells is causing the reduced VEGF levels in ascites.

We present the first evidence for efficacy of PG545 in OVCA. Increased heparanase activity has been associated with enhanced angiogenic and metastatic properties in renal cell, melanoma and hepatocellular carcinoma [38–42]. Given the extreme metastatic capability and dependence upon the VEGF-signaling pathway in OVCA [41], PG545 may be considered an ideal drug candidate for testing in this cancer indication. Moreover, increasing evidence has suggested a critical role for HB-EGF in ovarian cancer progression [43] as a negative prognostic factor [44]. Furthermore HB-EGF might be involved in tumour resistance against paclitaxel [45]. Inhibition of HB-EGF has recently been shown to overcome chemoresistance in ovarian cancer models [31]. Our *in vitro* data shows PG545 inhibits the migration and invasion of OVCA cells and decreased activation of the ERK/MAPK pathway through modulation of HB-EGF induced signaling and preliminary results indicate that PG545 modulates plasma HB-EGF levels in some cancer patients (Supplementary Fig. S6). Importantly, *in vivo* data using PG545 against various OVCA cells in immune-compromised and in immunocompetent models demonstrated significant anti-tumour activity of PG545 as a single agent and in combination with standard cytotoxic agents (platinum or taxane). More importantly, PG545 as a maintenance therapy significantly increases overall survival in these models.

This preclinical data provides a strong rationale to test PG545 as a single agent or in combination with standard chemotherapeutic agents, and in particular, paclitaxel in patients with OVCA.

Supplementary Material

Refer to Web version on PubMed Central for supplementary material.

Acknowledgements

The authors wish to acknowledge the technical assistance of Jacie Maguire, Takayo Ota, Jenifer Baranski, Erin Trchet (Charles River Discovery Service, Morrisville, NC), Kay Meshaw (Charles River Discovery and Imaging Services, Ann Arbor, MI) on the A2780 s.c. model, Ralf Brandt (vivoPharm, Bundoora, VIC, Australia) for the SKOV3 model, Maree Smith, Debra Siebert and Linda Wright (TetraQ, Brisbane, Australia) for the bioanalysis of the PG545 samples.

Role of Funding Source

The work conducted by the laboratory head Dr Viji Shridhar is supported in part by the grants from the National Institutes of Health CA123249, and Minnesota Cancer Alliance (MOCA) to (VS) and Gynecologic Oncology Fellowship fund to (BW) from the Department of Obstetrics and Gynecology at Mayo Clinic.

References

1. Gavalas NG, Lontos M, Trachana S-P, Bagratuni T, Arapinis C, Liacos C, et al. Angiogenesis-related pathways in the pathogenesis of ovarian cancer. *Int J Mol Sci.* 2013; 14:15885–909. doi: 10.3390/ijms140815885. [PubMed: 23903048]
2. Madsen CV, Steffensen KD, Olsen DA, Waldstrøm M, Smerdel M, Adimi P, et al. Serial measurements of serum PDGF-AA, PDGF-BB, FGF2, and VEGF in multiresistant ovarian cancer patients treated with bevacizumab. *J Ovarian Res.* 2012; 5:23. doi:10.1186/1757-2215-5-23. [PubMed: 22989094]
3. Yagi H, Miyamoto S, Tanaka Y, Sonoda K, Kobayashi H, Kishikawa T, et al. Clinical significance of heparin-binding epidermal growth factor-like growth factor in peritoneal fluid of ovarian cancer. *Br J Cancer.* 2005; 92:1737–45. doi:10.1038/sj.bjc.6602536. [PubMed: 15827558]
4. Davidson B, Shafat I, Risberg B, Ilan N, Trope' CG, Vlodaysky I, et al. Heparanase expression correlates with poor survival in metastatic ovarian carcinoma. *Gynecol Oncol.* 2007; 104:311–9. doi:10.1016/j.ygyno.2006.08.045. [PubMed: 17030350]
5. Zheng H, Ruan J, Zhao P, Chen S, Pan L, Liu J. Heparanase is involved in proliferation and invasion of ovarian cancer cells. *Cancer Biomark.* 2015 doi:10.3233/CBM-150459.
6. Parish CR, Freeman C, Hulett MD. Heparanase: a key enzyme involved in cell invasion. *Biochim Biophys Acta.* 2001; 1471:M99–108. [PubMed: 11250066]
7. Ramani VC, Purushothaman A, Stewart MD, Thompson CA, Vlodaysky I, Au JL-S, et al. The heparanase/syndecan-1 axis in cancer: mechanisms and therapies. *FEBS J.* 2013; 280:2294–306. doi:10.1111/febs.12168. [PubMed: 23374281]
8. Kjellén L, Lindahl U. Proteoglycans: structures and interactions. *Annu Rev Biochem.* 1991; 60:443–75. doi:10.1146/annurev.bi.60.070191.002303. [PubMed: 1883201]
9. Arvatz G, Shafat I, Levy-Adam F, Ilan N, Vlodaysky I. The heparanase system and tumor metastasis: is heparanase the seed and soil? *Cancer Metastasis Rev.* 2011; 30:253–68. doi:10.1007/s10555-011-9288-x. [PubMed: 21308479]
10. Sanderson RD. Heparan sulfate proteoglycans in invasion and metastasis. *Semin Cell Dev Biol.* 2001; 12:89–98. doi:10.1006/scdb.2000.0241. [PubMed: 11292374]
11. Sanderson RD, Yang Y, Suva LJ, Kelly T. Heparan sulfate proteoglycans and heparanase- - partners in osteolytic tumor growth and metastasis. *Matrix Biol.* 2004; 23:341–52. doi:10.1016/j.matbio.2004.08.004. [PubMed: 15533755]
12. Sasisekharan R, Shriver Z, Venkataraman G, Narayanasami U. Roles of heparan-sulphate glycosaminoglycans in cancer. *Nat Rev Cancer.* 2002; 2:521–8. doi:10.1038/nrc842. [PubMed: 12094238]

13. Dredge K, Hammond E, Davis K, Li CP, Liu L, Johnstone K, et al. The PG500 series: novel heparan sulfate mimetics as potent angiogenesis and heparanase inhibitors for cancer therapy. *Invest New Drugs*. 2010; 28:276–83. doi:10.1007/s10637-009-9245-5. [PubMed: 19357810]
14. Hammond E, Handley P, Dredge K, Bytheway I. Mechanisms of heparanase inhibition by the heparan sulfate mimetic PG545 and three structural analogues. *FEBS Open Bio*. 2013; 3:346–51. doi:10.1016/j.fob.2013.07.007.
15. Ferro V, Liu L, Johnstone KD, Wimmer N, Karoli T, Handley P, et al. Discovery of PG545: a highly potent and simultaneous inhibitor of angiogenesis, tumor growth, and metastasis. *J Med Chem*. 2012; 55:3804–13. doi:10.1021/jm201708h. [PubMed: 22458531]
16. Dredge K, Hammond E, Handley P, Gonda TJ, Smith MT, Vincent C, et al. PG545, a dual heparanase and angiogenesis inhibitor, induces potent anti-tumour and anti-metastatic efficacy in preclinical models. *Br J Cancer*. 2011; 104:635–42. doi:10.1038/bjc.2011.11. [PubMed: 21285983]
17. Hammond E, Brandt R, Dredge K. PG545, a heparan sulfate mimetic, reduces heparanase expression in vivo, blocks spontaneous metastases and enhances overall survival in the 4T1 breast carcinoma model. *PLoS One*. 2012; 7:e52175. doi:10.1371/journal.pone.0052175. [PubMed: 23300607]
18. Boyango I, Barash U, Naroditsky I, Li J-P, Hammond E, Ilan N, et al. Heparanase cooperates with Ras to drive breast and skin tumorigenesis. *Cancer Res*. 2014; 74:4504–14. doi:10.1158/0008-5472.CAN-13-2962. [PubMed: 24970482]
19. Aghajanian C, Blank S V, Goff BA, Judson PL, Teneriello MG, Husain A, et al. OCEANS: a randomized, double-blind, placebo-controlled phase III trial of chemotherapy with or without bevacizumab in patients with platinum-sensitive recurrent epithelial ovarian, primary peritoneal, or fallopian tube cancer. *J Clin Oncol*. 2012; 30:2039–45. doi:10.1200/JCO.2012.42.0505. [PubMed: 22529265]
20. Bookman MA. First-line chemotherapy in epithelial ovarian cancer. *Clin Obstet Gynecol*. 2012; 55:96–113. doi:10.1097/GRF.0b013e31824b45da. [PubMed: 22343232]
21. Dhillon S. Bevacizumab combination therapy: for the first-line treatment of advanced epithelial ovarian, fallopian tube or primary peritoneal cancer. *Drugs*. 2012; 72:917–30. doi:10.2165/11208940-000000000-00000. [PubMed: 22515620]
22. Integrated genomic analyses of ovarian carcinoma. *Nature*. 2011; 474:609–15. doi:10.1038/nature10166. [PubMed: 21720365]
23. Chien J, Aletti G, Baldi A, Catalano V, Muretto P, Keeney GL, et al. Serine protease HtrA1 modulates chemotherapy-induced cytotoxicity. *J Clin Invest*. 2006; 116:1994–2004. doi:10.1172/JCI27698. [PubMed: 16767218]
24. Roby KF, Taylor CC, Sweetwood JP, Cheng Y, Pace JL, Tawfik O, et al. Development of a syngeneic mouse model for events related to ovarian cancer. *Carcinogenesis*. 2000; 21:585–91. [PubMed: 10753190]
25. Chou T-C. Theoretical basis, experimental design, and computerized simulation of synergism and antagonism in drug combination studies. *Pharmacol Rev*. 2006; 58:621–81. doi:10.1124/pr.58.3.10. [PubMed: 16968952]
26. Van der Bilt ARM, van der Zee AGJ, de Vries EGE, de Jong S, Timmer-Bosscha H, ten Hoor KA, et al. Multiple VEGF family members are simultaneously expressed in ovarian cancer: a proposed model for bevacizumab resistance. *Curr Pharm Des*. 2012; 18:3784–92. [PubMed: 22591424]
27. Naora H. Heterotypic cellular interactions in the ovarian tumor microenvironment: biological significance and therapeutic implications. *Front Oncol*. 2014; 4:18. doi:10.3389/fonc.2014.00018. [PubMed: 24567915]
28. Ko SY, Naora H. Therapeutic strategies for targeting the ovarian tumor stroma. *World J Clin Cases*. 2014; 2:194–200. doi:10.12998/wjcc.v2.i6.194. [PubMed: 24945005]
29. Ostapoff KT, Awasthi N, Cenik BK, Hinz S, Dredge K, Schwarz RE, et al. PG545, an angiogenesis and heparanase inhibitor, reduces primary tumor growth and metastasis in experimental pancreatic cancer. *Mol Cancer Ther*. 2013; 12:1190–201. doi:10.1158/1535-7163.MCT-12-1123. [PubMed: 23696215]

30. Cole CL, Rushton G, Jayson GC, Avizienyte E. Ovarian cancer cell heparan sulfate 6-O-sulfotransferases regulate an angiogenic program induced by heparin-binding epidermal growth factor (EGF)-like growth factor/EGF receptor signaling. *J Biol Chem*. 2014; 289:10488–501. doi: 10.1074/jbc.M113.534263. [PubMed: 24563483]
31. Tang X, Deng S, Li M, Lu M. The anti-tumor effect of cross-reacting material 197, an inhibitor of heparin-binding EGF-like growth factor, in human resistant ovarian cancer. *Biochem Biophys Res Commun*. 2012; 422:676–80. doi:10.1016/j.bbrc.2012.05.052. [PubMed: 22609777]
32. Mabuchi S, Terai Y, Morishige K, Tanabe-Kimura A, Sasaki H, Kanemura M, et al. Maintenance treatment with bevacizumab prolongs survival in an in vivo ovarian cancer model. *Clin Cancer Res*. 2008; 14:7781–9. doi:10.1158/1078-0432.CCR-08-0243. [PubMed: 19047105]
33. Oliva P, Decio A, Castiglioni V, Bassi A, Pesenti E, Cesca M, et al. Cisplatin plus paclitaxel and maintenance of bevacizumab on tumour progression, dissemination, and survival of ovarian carcinoma xenograft models. *Br J Cancer*. 2012; 107:360–9. doi:10.1038/bjc.2012.261. [PubMed: 22713663]
34. Willett CG, Boucher Y, Duda DG, di Tomaso E, Munn LL, Tong RT, et al. Surrogate markers for antiangiogenic therapy and dose-limiting toxicities for bevacizumab with radiation and chemotherapy: continued experience of a phase I trial in rectal cancer patients. *J Clin Oncol*. 2005; 23:8136–9. doi:10.1200/JCO.2005.02.5635. [PubMed: 16258121]
35. Kobold S, Hegewisch-Becker S, Oechsle K, Jordan K, Bokemeyer C, Atanackovic D. Intraperitoneal VEGF inhibition using bevacizumab: a potential approach for the symptomatic treatment of malignant ascites? *Oncologist*. 2009; 14:1242–51. doi:10.1634/theoncologist.2009-0109. [PubMed: 20008305]
36. Pichelmayer O, Gruenberger B, Zielinski C, Raderer M. Bevacizumab is active in malignant effusion. *Ann Oncol*. 2006; 17:1853. doi:10.1093/annonc/mdl143. [PubMed: 16790519]
37. Ahmed N, Stenvers KL. Getting to know ovarian cancer ascites: opportunities for targeted therapy-based translational research. *Front Oncol*. 2013; 3:256. doi:10.3389/fonc.2013.00256. [PubMed: 24093089]
38. Chen G, Dang Y-W, Luo D-Z, Feng Z-B, Tang X-L. Expression of heparanase in hepatocellular carcinoma has prognostic significance: a tissue microarray study. *Oncol Res*. 2008; 17:183–9. [PubMed: 18773863]
39. Mikami S, Oya M, Shimoda M, Mizuno R, Ishida M, Kosaka T, et al. Expression of heparanase in renal cell carcinomas: implications for tumor invasion and prognosis. *Clin Cancer Res*. 2008; 14:6055–61. doi:10.1158/1078-0432.CCR-08-0750. [PubMed: 18809970]
40. Rivera RS, Nagatsuka H, Siar CH, Gunduz M, Tsujigiwa H, Han PP, et al. Heparanase and vascular endothelial growth factor expression in the progression of oral mucosal melanoma. *Oncol Rep*. 2008; 19:657–61. [PubMed: 18288398]
41. Trinh XB, Tjalma WAA, Vermeulen PB, Van den Eynden G, Van der Auwera I, Van Laere SJ, et al. The VEGF pathway and the AKT/mTOR/p70S6K1 signalling pathway in human epithelial ovarian cancer. *Br J Cancer*. 2009; 100:971–8. doi:10.1038/sj.bjc.6604921. [PubMed: 19240722]
42. Zetser A, Bashenko Y, Edovitsky E, Levy-Adam F, Vlodaysky I, Ilan N. Heparanase induces vascular endothelial growth factor expression: correlation with p38 phosphorylation levels and Src activation. *Cancer Res*. 2006; 66:1455–63. doi:10.1158/0008-5472.CAN-05-1811. [PubMed: 16452201]
43. Miyamoto S, Iwamoto R, Furuya A, Takahashi K, Sasaki Y, Ando H, et al. A novel anti-human HB-EGF monoclonal antibody with multiple antitumor mechanisms against ovarian cancer cells. *Clin Cancer Res*. 2011; 17:6733–41. doi:10.1158/1078-0432.CCR-11-1029. [PubMed: 21918176]
44. Tanaka Y, Miyamoto S, Suzuki SO, Oki E, Yagi H, Sonoda K, et al. Clinical significance of heparin-binding epidermal growth factor-like growth factor and a disintegrin and metalloprotease 17 expression in human ovarian cancer. *Clin Cancer Res*. 2005; 11:4783–92. doi: 10.1158/1078-0432.CCR-04-1426. [PubMed: 16000575]
45. Yagi H, Yotsumoto F, Sonoda K, Kuroki M, Mekada E, Miyamoto S. Synergistic anti-tumor effect of paclitaxel with CRM197, an inhibitor of HB-EGF, in ovarian cancer. *Int J Cancer*. 2009; 124:1429–39. doi:10.1002/ijc.24031. [PubMed: 19048624]

Highlights

1. In combination with paclitaxel, PG545 showed synergy against A2780 cells.
2. PG545 inhibited signalling and reduced growth factor-mediated cell migration.
3. Efficacious alone or in combination with chemotherapies in A2780 and SKOV-3 models.
4. Increased survival in chemotherapy maintenance model has clinical ramifications.
5. Evidence of biomarker response in preclinical and clinical studies.

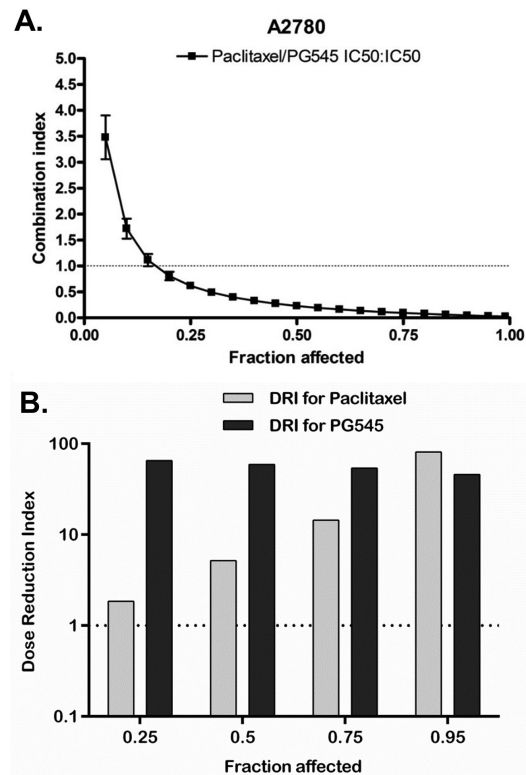


Figure 1. Combination of PG545 and paclitaxel against A2780 cells was analysed for synergy using the method of Chou-Talalay. **A.** The fraction affected (Fa) and Combination Index (CI) values were calculated and plotted using Calcsyn software after the combined action of Paclitaxel: PG545 (0.09375:7.125 μ M) in A2780 cell for 48h. **B.** DRI for PG545 and paclitaxel was plotted against Fa.

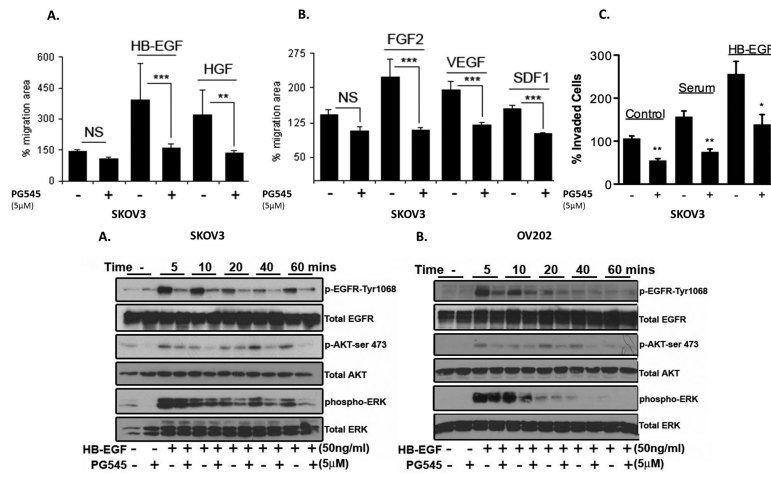


Figure 2. PG545 significantly inhibits migration and invasion of SKOV3 ovarian cancer cells by targeting growth factors. **A** and **B**. PG545 (5µM) significantly inhibited migration of SKOV3 ovarian cancer cells stimulated by each of the following HS binding growth factors: HB-EGF, HGF, FGF-2, VEGF₁₆₅ and SDF-1. **C**. PG545 was also tested against HB-EGF-dependent SKOV3 cell invasion and the compound was found to be a potent inhibitor of this process. NS: Not significant; *p<0.05, **p<0.01, ***p<0.001. **D** and **E**. After the SKOV3 cells (**D**) or OV202 (**E**) were cultured in 0.2% serum containing medium for 12hrs, 50ng/ml HB-EGF was added with and without PG545 for the indicated times. Western blot analysis indicated diminished phosphorylation of EGFR, ERK and AKT. Total EGFR, ERK and AKT are shown for equal loading.

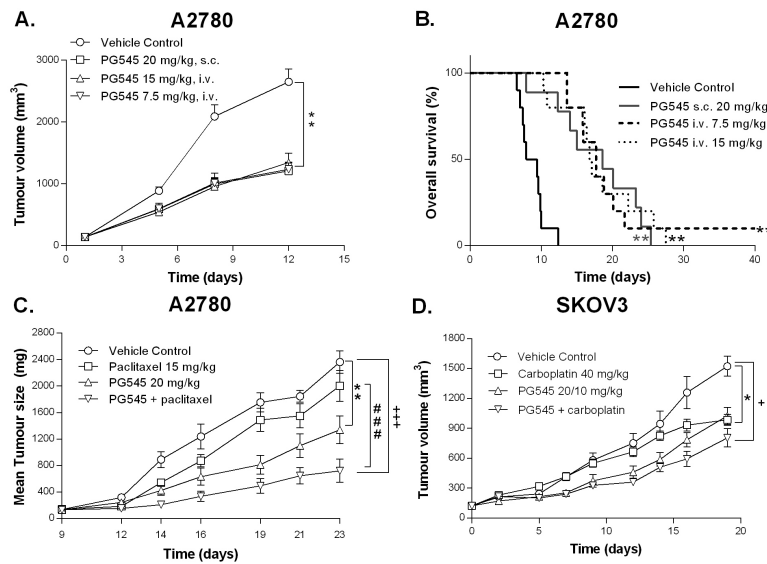


Figure 3.

Combination treatment using xenograft models. **A.** PG545 administered either s.c. or i.v. in the A2780 model. Treatment started on day 1 ($n = 10/\text{group}$) using 20mg/kg s.c. (1x/wk \times 3), 7.5mg/kg i.v. (2x/wk \times 3) or 15mg/kg i.v. (1x/wk \times 3) when the tumour mean volumes were 140mm³. Efficacy was determined from tumour growth inhibition (TGI) estimated at 55%, 45%, and 55% for 20mg/kg s.c., 15mg/kg i.v. and 7.5mg/kg i.v., respectively on day 12. All treatment groups were considered significant compared versus vehicle control ($p < 0.01$). **B.** PG545 treated animals survived ~ 2.5 times longer compared to untreated controls (** $p < 0.01$, log-rank test). **C.** A2780 cells were injected s.c. and treatment started with paclitaxel once mean estimated tumour mass reached 136mg. Two days post-paclitaxel treatment, PG545 was administered and treatment continued for 3 weeks. Tumour Growth Inhibition (TGI) for paclitaxel, PG545 and the paclitaxel/PG545 combination group was 11%, 48% and 79% respectively. **D.** SKOV3 cells were injected s.c. and treatment started at 37 days when the average tumour volume was approximately 123mm³. Vehicle control and PG545 were administered once weekly, s.c. and carboplatin (40 mg/kg) was administered i.v. once weekly. The dose of PG545 was reduced from 20 to 10mg/kg after the first dose. In the groups receiving combination therapy, PG545 was administered two days after carboplatin. TGI at Day 19 was estimated at 40% for PG545 alone, 43% carboplatin alone and 58% for the combination. One mouse in the combination group was culled due to excess bodyweight on Day12 of the study. Otherwise, the combination was well tolerated (a combination arm using 60 mg/kg carboplatin led to TGI of 73% but also bodyweight loss in two mice which were culled in Day 12, data not shown). *= $p < 0.05$, **= $p < 0.01$ PG545 alone versus vehicle control, ### = $p < 0.001$ PG545 and paclitaxel combination versus paclitaxel alone, and + = $p < 0.05$, +++ = $p < 0.001$ combination groups versus vehicle control.

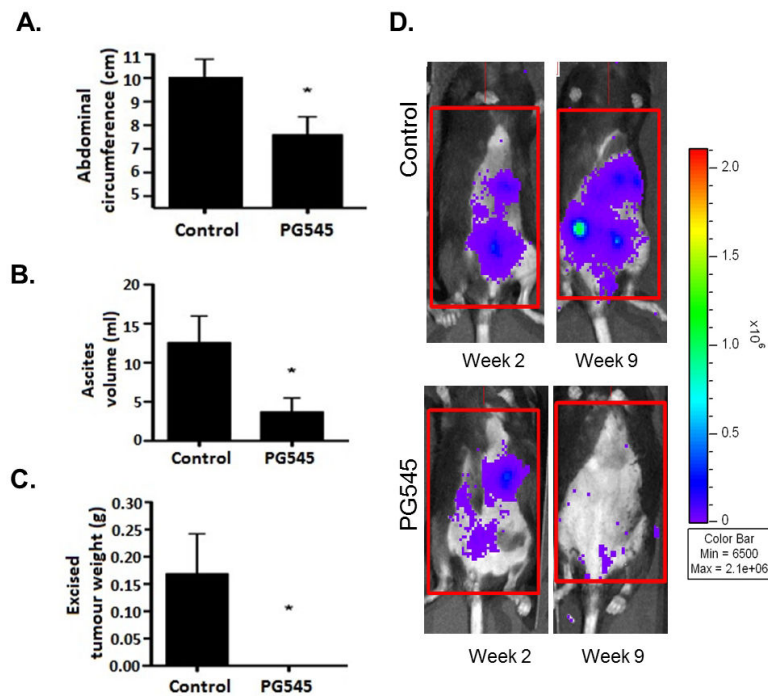


Figure 4.

Significant anti-tumour activity of PG545 in the immunocompetent ID8 ovarian cancer model. Twenty mice were injected i.p. with 5×10^6 ID8 cells. Three days after inoculation, mice were randomized to two different groups of 10 mice/grp: **1.** control (i.p. PBS), **2.** PG545 20mg/kg/wk i.p. for 10 wks. Abdominal circumference (**A**), volume of ascites (**B**), and total excised tumour weight (**C**) was then calculated for each treatment group and compared to control $*=p<0.05$. **D.** Representative images of control and PG545-treated mice in week 2 and week 9 in ID8 tumour-bearing mice using the IVIS luminescence imaging system series 2000. Color bar shows photon intensity.

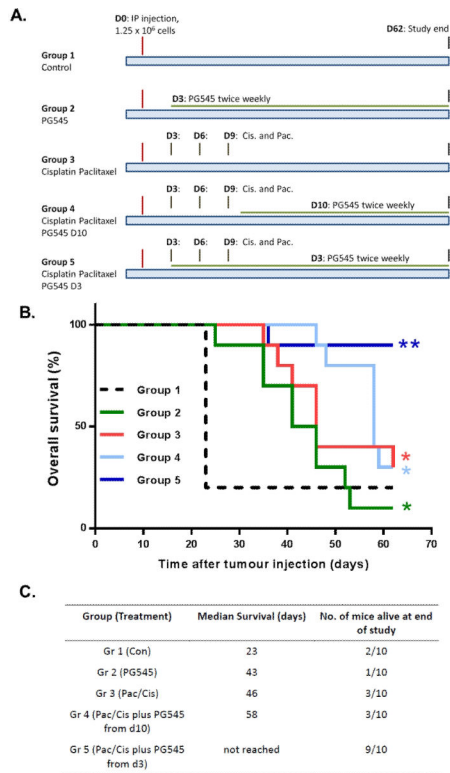


Figure 5.

Combination effect of PG545, cisplatin, paclitaxel in A2780 model. **A.** Fifty mice were injected i.p. with 1.25 × 10⁶ A2780 cells and randomly assigned to 5 treatment groups. Treatment with drugs commenced on Day 3. Group 1: Vehicle control, Group 2: PG545 20mg/kg twice a week starting at day 3 and maintained till the end of the study, Group 3: cisplatin 6mg/kg and paclitaxel 15mg/kg on days 3, 6 and 9 only. Group 4: Cisplatin and paclitaxel (days 3, 6 and 9) PG545 20mg/kg twice a week starting on day 10 and continued until the end of the experiment. Group 5: Cisplatin and paclitaxel (days 3, 6 and 9) PG545 20mg/kg twice a week starting on day 3 and continued until the end of the experiment. **B.** Kaplan Meier survival curves reveal the significant enhancement of survival following treatment with PG545 alone, doublet therapy of paclitaxel/cisplatin or triplet therapy of PG545/paclitaxel/cisplatin on days as indicated. * = P < 0.05, ** = P < 0.01. **C.** Median survival in days and number of mice alive at the end of the study are shown in the various treatment groups.

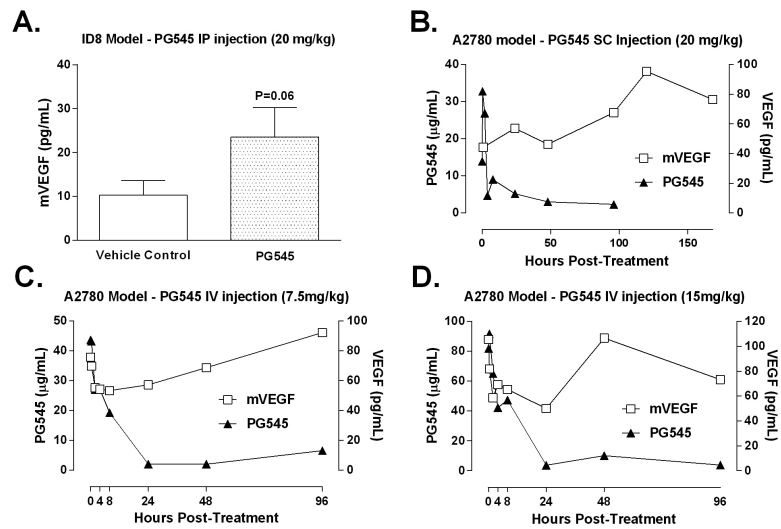


Figure 6.

Increased plasma VEGF is a putative pharmacodynamic marker following treatment *via* different routes of administration with PG545 in preclinical studies. Preliminary yet robust data were generated from the immunocompetent ID8 model and the immunodeficient A2870 model. **A.** Plasma VEGF concentration was increased in the PG545- treated group (IP injection) versus control animals with borderline statistical significance ($P=0.06$). **B-D.** Time versus concentration profiles for PG545 (black triangles) was determined following administration of either via SC injection (20 mg/kg), or IV injection (7 or 15 mg/kg) led to increases in plasma VEGF concentration (open squares).

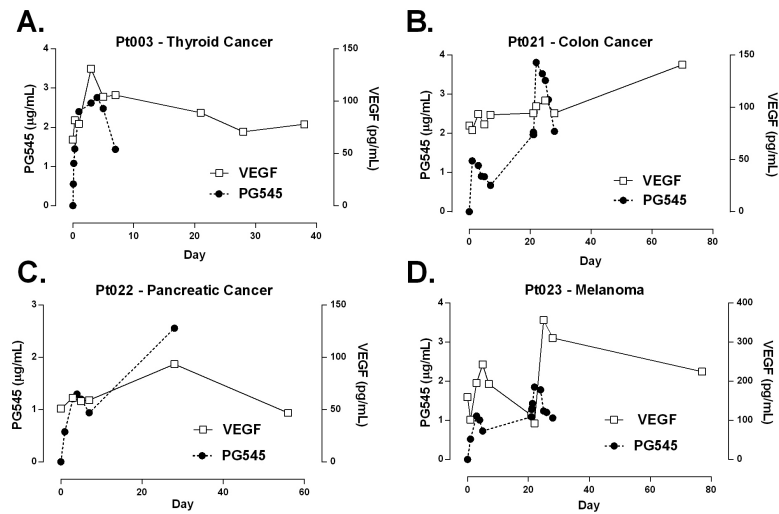


Figure 7.

Treatment with PG545 increases plasma VEGF levels in patients with solid tumours.

Administration with weekly s.c. injections of PG545 leads to increases in plasma VEGF (white squares). PG545 plasma concentrations are indicated by the black circles. Patient Pt003 (thyroid) received 2 doses of 50mg of PG545 and the other three patients (colon, pancreatic, and melanoma) received 7, 3 and 8 doses of 25mg respectively. Dosing regimen: Pt003: days 0, 7; Pt021: days 0, 7, 14, 21, 28, 35, 42; Pt022: days 0, 7, 14; Pt023: days 0, 7, 14, 21, 28, 35, 42, 49.